Technical Report

Gain Measurement of the Sinarback 54 Digital Camera

February 11, 2005

Mahdi Nezamabadi

Spectral Color Imaging Laboratory Group
Munsell Color Science Laboratory
Chester F. Carlson Center for Imaging Science
Rochester Institute of Technology

mxn9911@cis.rit.edu
http://www.art-si.org/

1. Abstract

The camera gain of a Sinarback 54 digital camera was measured and found to be 6.0 electrons / digital count. The camera is designed in such a way that it can use 98% of the nominal full well capacity of its CCD. A linear relationship was found between integration times and mean digital counts of dark current images.

2. Introduction

Understanding the building blocks of digital camera acquisition is important for determining the system gain and noise characteristics. Optics focus an image of the scene on the image plane of the camera where, in this case, a CCD chip is located. Photons emitted from scene interact with the CCD's silicon lattice and are sometimes absorbed releasing energy that promotes electrons from their position within the structure into the conduction band where they travel freely. The freed electrons can become entrapped in pixel potential wells. Peripheral CCD electronics will create a voltage based on the charge collected in a pixel. The analog signal will later be converted to a digital signal via Analog-to-Digital Converter (ADC) circuitry. Camera gain is the number of electrons required to increment digital count by one unit. An experiment was performed to measure camera gain for Sinarback 54 digital camera. This Sinarback 54 is currently used in spectral imaging lab at Munsell Color Science Laboratory (MCSL) at RIT.

The heart of Sinarback 54 digital camera is a Kodak KAF-22000CE Image Sensor with 4080x5440 pixels. This is a full-frame color image sensor with 9μm x 9μm pixels. Each pixel is covered by one of the red, green, or blue filters. The Red, green, and blue pixels are arranged based on a Bayer pattern, as depicted in Figure 1; so, the number of green pixels is twice the number of red or blue pixels. The Sinar CaptureShop 4.0.21 software was used to drive the camera in single-shot mode. This software has its own internal interpolation algorithm for deriving RGB values at each pixel. Such post processing can affect the results of gain calculations and other characteristic factors of the camera. To avoid confounding the experimental results, only raw output files were analyzed. Sinar CaptureShop was not utilized for interpolation or other image processing.

The Sinarback 54 camera has a 14-bit ADC circuit, so output digital counts are in the range of 0 to 16383 (2^{14}-1=16383). The full specification of the Kodak KAF-22000CE CCD is available at reference [1].

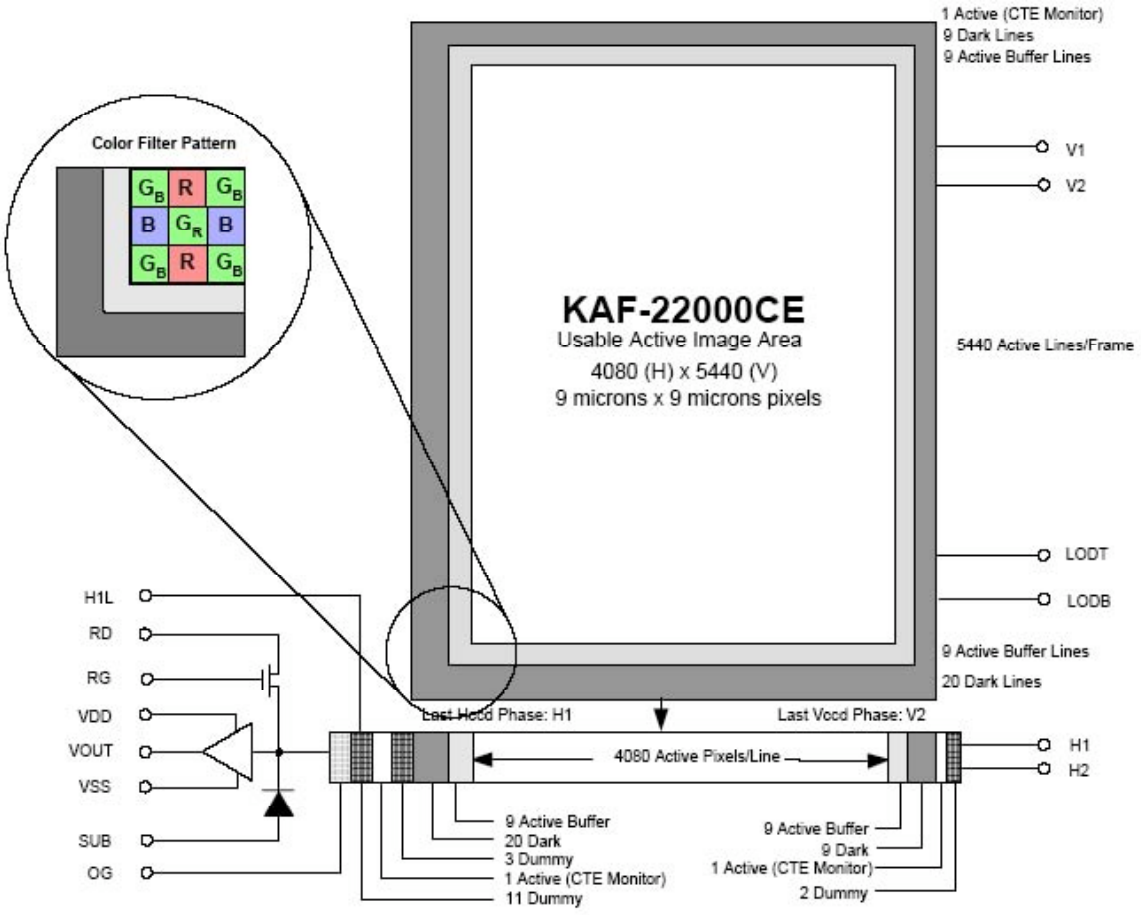

Figure 1- Distribution of red, green, and blue pixels according to Bayer pattern [1].

3. Camera Noise

Noise in image sensors can be classified into two main categories, random noise and pattern noise [2].

3.1. Random noise

Random noise varies frame to frame in the image and is reduced by averaging successive frames. Photon noise is a component of random noise. It is due to the intrinsic

characteristics of how photons are emitted from a light source. Photonic noise is also known as shot noise and is statistically well described by the Poisson distribution. Other examples of random noise are reset noise, amplifier noise, and 1/f noise. Figure 2-a through 2-g present ideal noiseless output signal and noisy signal due to different sources of noise.

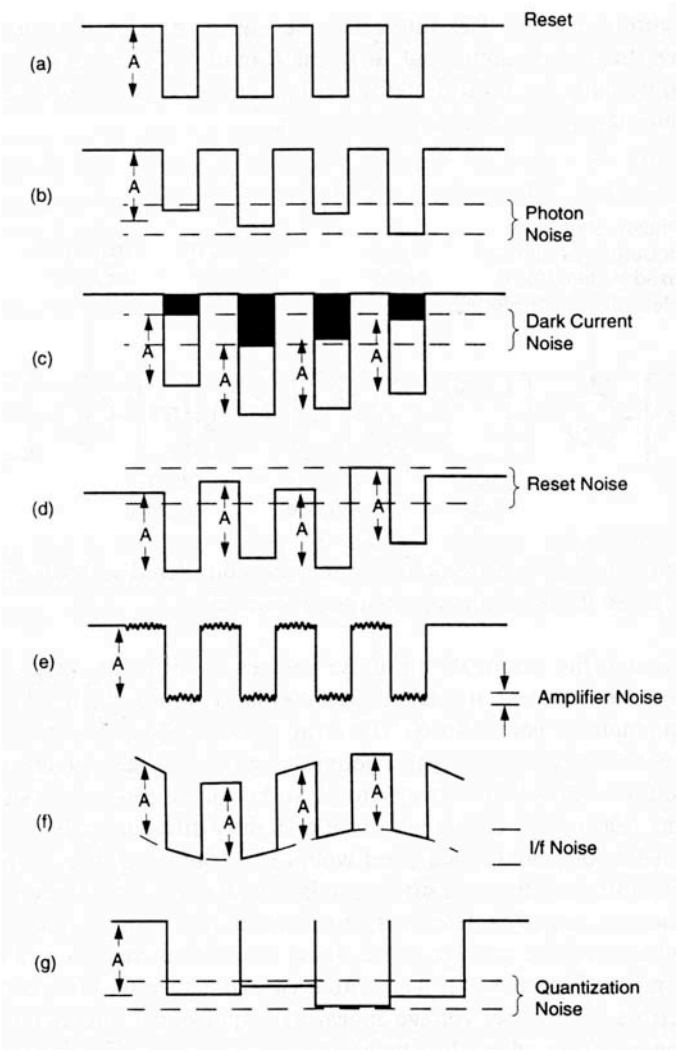

Figure 2- Ideal noiseless signal (a) and noisy signals (b) to (g) due to different sources of noise [2].

3.2. Pattern noise

Pattern noise is a spatial noise that does not change significantly from frame to frame. This type of noise is mainly due to variation factors such as detector dimension, doping concentrations, contamination, and thickness changes of overlayers. Fixed pattern noise

(FPN) and photo-response non-uniformity (PRNU) are two typical examples of pattern noise. Dark current noise is another example of FPN. Frame averaging does not reduce pattern noise. Figure 3 illustrates signal transfer steps and different sources of noise involved at each step. It is understood that the noise magnitude is the root mean square (RMS) of the random process producing the noise [2]. In other words, noise powers are considered additive, that is, the noise sources are added in squared form, as presented in equation (1).

$$\sigma_{system}^2 = \sigma_{shot}^2 + \sigma_{pattern}^2 + \sigma_{on-chip}^2 + \sigma_{off-chip}^2 + \sigma_{ADC}^2 \qquad (1)$$

Where σ_{system}^2 is the square of the total noise of the system, and σ_{shot}^2, $\sigma_{pattern}^2$, $\sigma_{on-chip}^2$, $\sigma_{off-chip}^2$, and σ_{ADC}^2 designate squares of shot noise, pattern noise, on-chip amplifier noise, off-chip amplifier noise, and analog-to-digital converter (ADC) noise respectively.

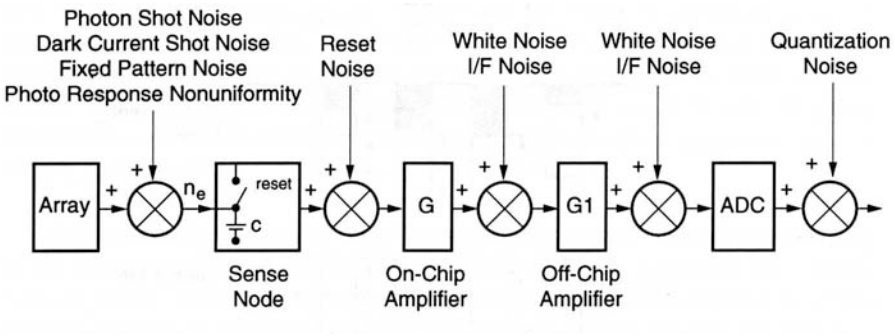

Figure 3- The various subsystems are considered ideal elements with the noise introduced at appropriate locations [2].

4. Camera Gain

Let us define camera gain, γ, as the number of electrons required to increase one unit in output digital count. Therefore a signal level in electron unit, *S*, is a product of gain, γ (electrons/digital count), and digital count, *D*, as presented in equation (3).

$$S = \gamma \cdot D \qquad (3)$$

Hence, the variance of signal will be proportional to variance of digital count with the square of camera gain proportionality constant, shown in equations (4) to (5).

$$VAR[S] = VAR[\gamma \cdot D] \tag{4}$$

$$\sigma_S^2 = \gamma^2 \cdot \sigma_D^2 \Leftrightarrow \frac{1}{\gamma^2} \cdot \sigma_S^2 = \sigma_D^2 \tag{5}$$

Combining equations (1) and (5) and dividing both sides by γ^2 we get equation (6), where variance of digital count, $\sigma_{D_{system}}^2$, is in linear relationship to the summation of noise components of the system by the inverse of the camera gain as a linear coefficient factor.

$$\sigma_{D_{system}}^2 = \frac{1}{\gamma^2}(\sigma_{shot}^2 + \sigma_{pattern}^2 + \sigma_{on-chip}^2 + \sigma_{off-chip}^2 + \sigma_{ADC}^2) \tag{6}$$

Photon noise is due to random arrival of photons on the CCD surface and is designated by $\sigma_{D_{photon}}$. Dark current noise, $\sigma_{D_{dark}}$, is due to random generation of electrons in an image captured in dark condition (closed shutter). Dark current average can be subtracted from the signal to eliminate the contribution of the dark signal, however, dark current noise cannot be eliminated [2]. Equation (6) can be rewritten as equation (7).

$$\sigma_{D_{system}}^2 = \frac{1}{\gamma^2}\sigma_{photon}^2 + \frac{1}{\gamma^2} \cdot (\sigma_{dark}^2 + \sigma_{pattern}^2 + \sigma_{on-chip}^2 + \sigma_{off-chip}^2 + \sigma_{ADC}^2) \tag{7}$$

It is often assumed that photon arrival on the CCD surface have Poisson distribution. The equation for this is shown in equations (8) and (9).

$$VAR[S_{photon}] = E[S_{photon}] = E[\gamma \cdot D_{photon}] \tag{8}$$

$$\sigma_{photon}^2 = \overline{S}_{photon} = \gamma \cdot \overline{D}_{photon} \tag{9}$$

Substituting equation (9) in equation (7) results in equation (10).

$$\sigma_{D_{system}}^2 = \frac{1}{\gamma} \cdot \overline{D}_{photon} + \frac{1}{\gamma^2} \cdot (\sigma_{dark}^2 + \sigma_{pattern}^2 + \sigma_{on-chip}^2 + \sigma_{off-chip}^2 + \sigma_{ADC}^2) \tag{10}$$

Equation (10) states that for different signal levels, variance of digital counts versus mean digital count of images is a linear curve with 1/γ as its gain factor. Therefore by capturing images at different amount of light incident on CCD and plotting variance of digital count of each image versus mean value of digital count for the corresponding image, one can estimate camera gain.

5. Experimental

A tablet of Polytetrafluoroethylene (PTFE) powder was made and used as a white sample, known as Halon (for further information on Halon preparation see [3]). Halon is a near perfect diffuser; its reflectance factor is almost equal to one for the range of the visible spectrum. A pair of tungsten hot-lights, Elinchrom Scanlite 1000, was used to illuminate the Halon sample. Images with different exposure times were captured. Figure 4 shows the relative spectral power distribution of Elinchrom Scanlite 1000. The light sources were located at approximately 45 degrees relative to the perpendicular axis of the Halon plane. The Sinarback 54 digital camera was equipped with an IR-cut off filter and a lens with a focal length of 100mm in the light path. The f-stop was set to f/22 and the camera was placed in the single-shot mode. All software post processing such as color balance and ISO correction was deactivated. The Sinarback 54 camera has a limited set of discrete exposure time values. The in-between steps of exposure levels were achieved by changing distance between the Halon sample and the light sources. Experimental arrangement is schematically presented in figure 5. At 45 levels of exposure two successive images were captured for a total of 90 images. The difference of each pair was calculated and saved. In this way the effect of dark current image was eliminated. It should be noted that the variance of digital counts of the difference of two successive images is half of the variance of the digital counts of each image (assuming that two images have the same mean values).

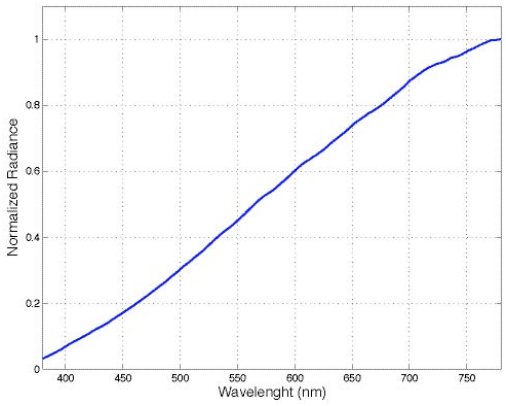

Figure 4- Relative spectral power distribution of Elinchrom Scanlite 1000.

In order to investigate the relationship between exposure time and dark current noise, 13 images were captured while the camera shutter was closed. Table 1 presents 13 exposure time values in seconds used in the dark current imaging.

Table 1- Exposure time values in seconds corresponding to the dark images.

Time (s)	0.125	0.250	0.500	1.000	2.000	4.000	8.000
	12.000	16.000	20.000	24.000	28.000	32.000	

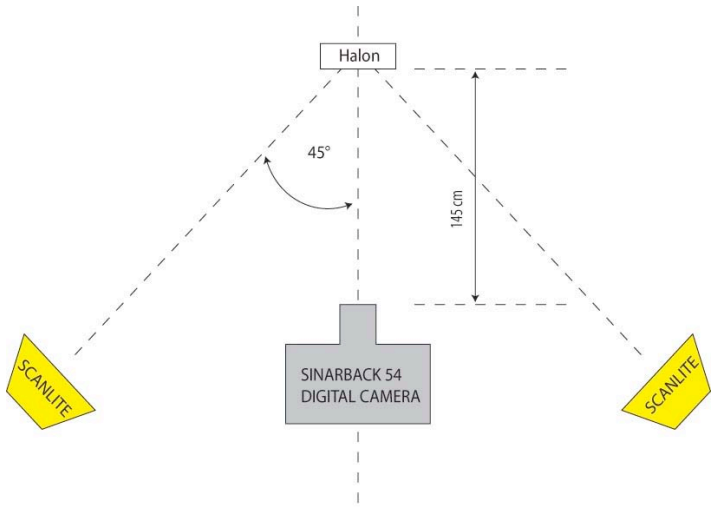

Figure 5- Equipment setup in imaging of the Halon sample.

6. Results and Discussion

Figure 6 presents the mean of digital counts versus variance in images taken with different amount of lights. As can be seen from Figure 6, most points for all three channels have aligned on the same line. However, there are points that are significantly off the line. All saturated pixels have values of 16383 with zero variance. It is understood that when a potential well fills, further collected charge can spill into adjacent pixels. This effect is known as blooming [4]. It was hypothesized that points on the Figure 6 curve that deviate from the straight line would correspond to light levels where at least one color channel was saturated. This hypothesis was examined by eliminating points with one or two channels that had a mean digital count of 10000 or more. The results are

illustrated in Figure 7. These points were corresponding to exposure values that cause red channel to bloom and charges spilled over into green and blue channels. This also indicated that the red channel was saturated before the green and blue channels, which is in accordance to higher quantum efficiency of the red channel (please refer to Kodak KAF-22000CE specification sheet) and higher relative power at long wavelengths for the light source. Furthermore long wavelength photons have longer absorption depth than short wavelength photons; hence, electrons generated by them are more probable to end in adjacent pixels during their random walk, than electrons generated by short wavelength photons. Therefore significant deviation from linear relationship in the high levels of signal can be attributed mainly to the blooming effect of the red channel.

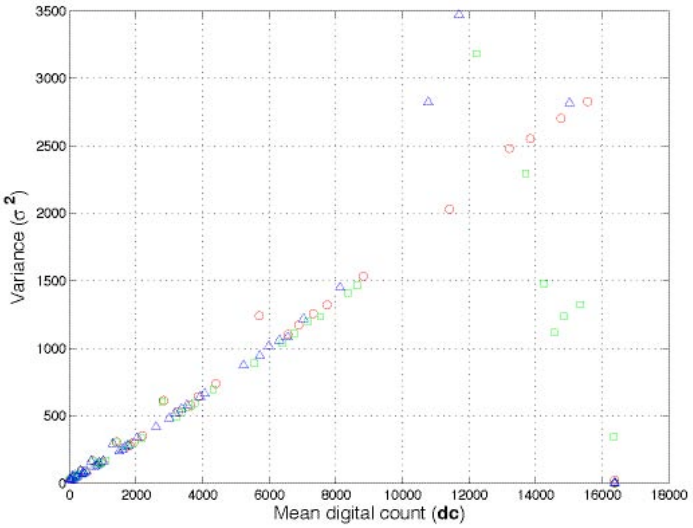

Figure 6- Mean digital counts of images captured with different exposures versus 1/2 of variance of digital counts of difference of two successive images. Red circles, green squares, and blue triangles denote for red, green, and blue channels respectively.

As described in section 5, by linear curve fitting of mean digital count versus variance of digital counts, one can calculate camera gain. Figure 8 illustrates linear regression result for measured data. As can be seen from Figure 8, there is a strong linear relationship, which is also confirmed by correlation coefficient, R^2, which is very close to one. The camera gain is estimated as 6.0 electrons / digital count. The number of electrons required to saturate a channel can be estimated by multiplication of maximum digital count and camera gain, that is 98298 electrons, (16383x6=98298). As stated in

Kodak KAF-22000CE specification sheet, full well capacity of the CCD is 100000 electrons. Hence the camera uses about 98% of full well capacity.

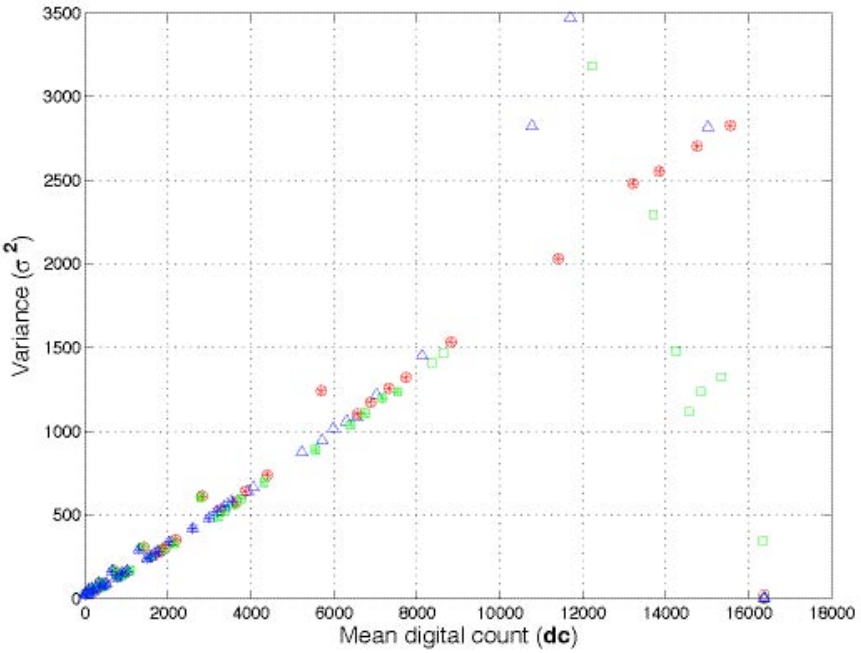

Figure 7- Mean digital counts of images captured with different exposures versus 1/2 of variance of digital counts of difference of two successive images. Red circles, green squares, and blue triangles denote for red, green, and blue channels respectively. Points without stars on their symbols are points with at least one saturated channel.

Figure 9 presents the mean digital counts of dark images versus integration time. As it can be seen, there is a linear relationship between integration time and mean digital count of dark images. The calculated R^2 for this linear regression is 0.9999.

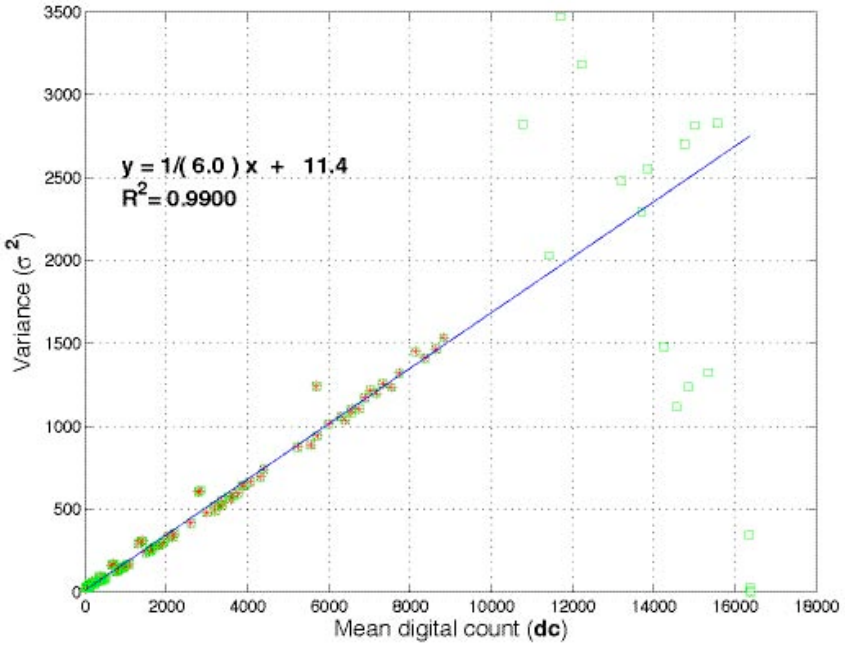

Figure 8- Linear regression of mean digital counts of images captured with different exposures versus 1/2 of variance of digital counts of difference of two successive images. Camera gain is estimated as 6.0 electrons / digital count. Points without stars on their symbols have not been used in linear regression.

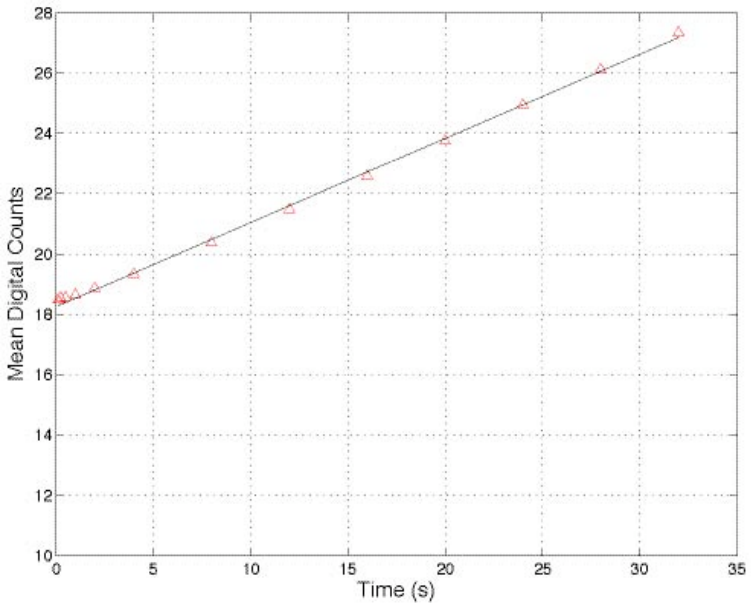

Figure 9- Mean digital count of dark images versus integration time.

7. Conclusion

Camera gain of Sinarback 54 digital camera was measured and found to be 6.0 electrons per digital count. The camera uses 98% of full well capacity of the CCD. The red channel was saturated before the green and blue channels. A linear relationship was found between integration times and mean digital count of dark current images.

8. Reference:

1- Full specification of Kodak KAF-22000CE Image Sensor can be found at: http://www.kodak.com/global/en/digital/ccd/products/fullframe/KAF-22000CE/evalBoard.jhtml.

2- Gerald C. Holst, *CCD Arrays, Cameras and Displays*, SPIE Optical Engineering Press, (1998), chapter 4.

3- Victor R. Weidner, Jack J. Hsia, Reflection Properties of Pressed Polytetrafluoroethylene Powder, J. Opt. Soc. Am., Vol. 71, No. 7, July 1981, F1-F6.

4- James R. Janesick, Scientific Charge-Coupled Devices, SPIE Press, (2001), chapter 2.